Provided for non-commercial research and education use.
Not for reproduction, distribution or commercial use.

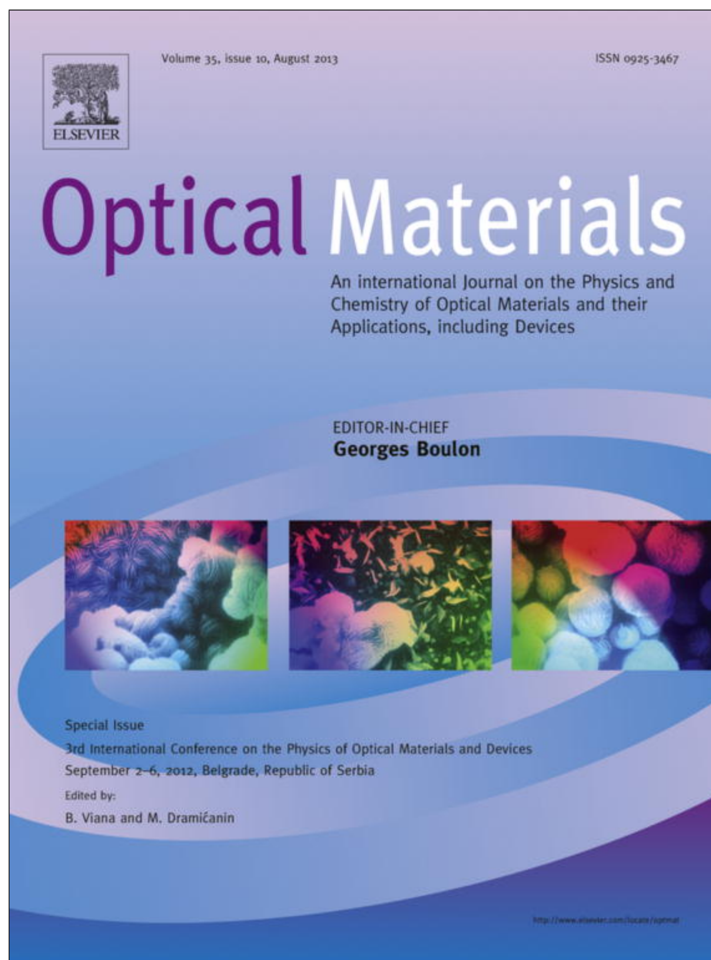

This article appeared in a journal published by Elsevier. The attached copy is furnished to the author for internal non-commercial research and education use, including for instruction at the authors institution and sharing with colleagues.

Other uses, including reproduction and distribution, or selling or licensing copies, or posting to personal, institutional or third party websites are prohibited.

In most cases authors are permitted to post their version of the article (e.g. in Word or Tex form) to their personal website or institutional repository. Authors requiring further information regarding Elsevier's archiving and manuscript policies are encouraged to visit:

http://www.elsevier.com/authorsrights

Author's personal copy

Optical Materials 35 (2013) 1829–1833

Contents lists available at SciVerse ScienceDirect

Optical Materials

journal homepage: www.elsevier.com/locate/optmat

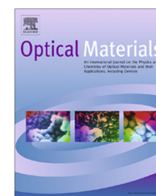

Luminescence studies in $In_xGa_{1-x}N$ epitaxial layers with different indium contents

T.Y. Wu [a], C.C. Chang [a], K.K. Tiong [a], Y.C. Lee [b,*], S.Y. Hu [c], L.Y. Lin [d], T.Y. Lin [d], Z.C. Feng [e]

[a] *Department of Electrical Engineering, National Taiwan Ocean University, Keelung, Taiwan*
[b] *Department of Electronic Engineering, Tungnan University, Shenkeng, New Taipei City, Taiwan*
[c] *Department of Electrical Engineering, Tungfang Design University, Kaohsiung, Taiwan*
[d] *Institute of Optoelectronic Sciences, National Taiwan Ocean University, Keelung, Taiwan*
[e] *Graduate Institute of Electro-Optical Engineering and Department of Electrical Engineering, National Taiwan University, Taipei, Taiwan*

A R T I C L E I N F O

Article history:
Available online 17 April 2013

Keywords:
InGaN
Temperature-dependent photoluminescence
Scanning Electron Microscopy

A B S T R A C T

The optical properties of $In_xGa_{1-x}N$ epitaxial layers ($x = 0.02$, 0.04, 0.11, 0.15, 0.30 and 0.33) grown by metalorganic chemical vapor deposition (MOCVD) have been investigated by temperature-dependent photoluminescence (PL) measurement. The surface morphologies of InGaN samples are studied by scanning electron microscopy (SEM) images. The PL feature at 12 K has shown an increase in full-width at half-maximum (FWHM) with increasing In content. An anomalous S-shaped temperature dependence of the PL peak energy exhibited by InGaN films with higher In content enabled the evaluation of the exciton localization energy. The broadened FWHM and S-shaped emission shift are attributed to larger compositional fluctuation due to compositional inhomogeneity of In. Additionally, the luminescence mechanism relating to the phase separation has to be considered for the much larger FWHM value and the pronounced S-shaped behavior for the InGaN samples with In content of 0.30 and 0.33.

© 2013 Elsevier B.V. All rights reserved.

1. Introduction

Recently, devices based on III-nitride compound semiconductors which include GaN, InGaN, and AlGaN materials have been rapidly and widely developed for highly efficient laser diodes, high brightness light emitting diodes (LEDs), photodetectors, etc. [1–4]. Among the III-nitride compound semiconductors, the direct band-gap InGaN-based semiconductors have attracted much attention for versatile optoelectronic device application because the energy gap can be tuned in a rather wide range from 3.4 eV for GaN in the ultraviolet (UV) region to 0.7 eV for InN in the infrared (IR) region [5,6]. However, the big difference in the covalent radii of In and Ga would result in inhomogeneous In distribution in InGaN films with higher In content, affecting the optical properties of the InGaN sample [6].

Up to date, several luminescence properties have been discussed for InGaN alloy semiconductor. It has been reported that the compositional fluctuation is one of the most important subjects with respect to the optical emission in InGaN alloys [7–10]. The compositional fluctuation has been known to be responsible for the broadening in the full-width at half-maximum (FWHM) of the luminescence feature and the observed 'S-shaped' temperature dependence of luminescence peak energy (red–blue–redshift with increasing temperature) relating to the exciton localization effect [11–14]. However, to our knowledge, detailed discussion concerning the relationship between the variation in FWHM and S-shaped emission shift for the InGaN with different In contents has not been well established.

In this work, we have investigated the luminescence properties of $In_xGa_{1-x}N$ grown by metalorganic chemical vapor deposition (MOCVD), as a function of x ($x = 0.02$, 0.04, 0.11, 0.15, 0.30 and 0.33). The temperature-dependent photoluminescence (PL) were measured to determine the dependence of the band-gap energy of InGaN on the In composition. The FWHM values and temperature-dependent peak energy of PL spectra taking into account the exciton localization effect are analyzed and discussed.

2. Experimental procedures

The $In_xGa_{1-x}N$ films investigated were grown by MOCVD system. On (1000) sapphire, a thin, about 30-nm thick, GaN buffer was first grown at low temperature (LT) at 530 °C, followed by approximately 1 μm thick GaN deposited at 1030 °C and finally followed by a nearly 100 nm thick InGaN layer grown at 700 °C. The composition values of these samples were determined by high resolution X-ray diffraction. Growth details of the samples can be found in Refs. [15,16]. The surface morphologies of InGaN samples observed by scanning electron microscopy (SEM) images were taken on a JEOL-JSM7001F. Temperature-dependent photolumines-

* Corresponding author. Tel.: +886 2 86625911x265; fax: +886 2 26629592.
E-mail address: jacklee@mail.tnu.edu.tw (Y.C. Lee).

0925-3467/$ - see front matter © 2013 Elsevier B.V. All rights reserved.
http://dx.doi.org/10.1016/j.optmat.2013.03.024

Author's personal copy

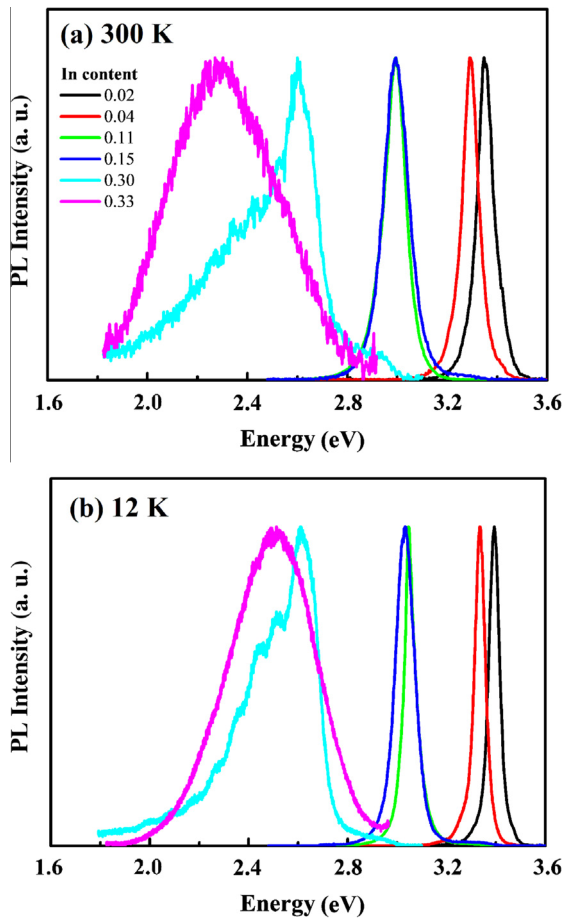

Fig. 1. PL spectra for the $In_xGa_{1-x}N$ films with different In contents measured at: (a) 300 K, and (b) 12 K.

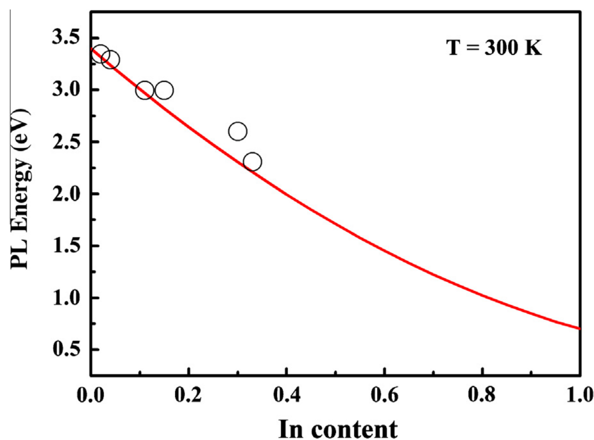

Fig. 2. Band-gap of the $In_xGa_{1-x}N$ films as a function of In content. The solid line is the fitted curve from Eq. (1).

cence (PL) measurements were conducted under the excitation with a 5 mW/cm^2 of a microchip laser (266 nm). The luminescence was collected using a spectrometer (Zolix omni-λ 500) with a 1200 grooves/mm grating and detected using a GaAs photomultiplier tube. The PL signal obtained from the photomultiplier was analyzed using lock-in technique and recorded in a computer. In addition, Janis Research Model CCS-150 and LakeShore Model 321 temperature controller were used to measure the PL spectrum as a function of temperature. The computational parts for the theoretical calculation in the present work are facilitated by commercially available Mathcad software.

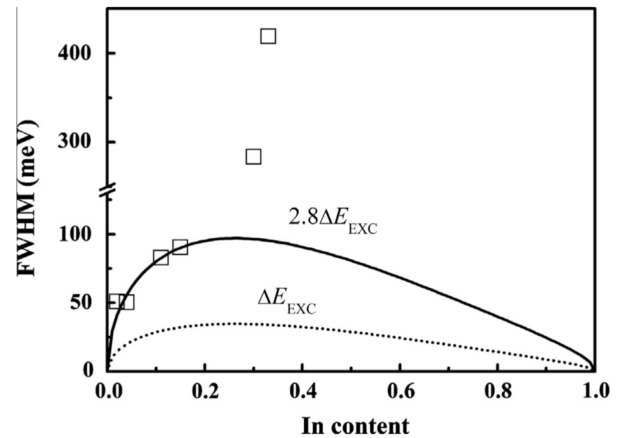

Fig. 3. The variation of the 12 K PL FWHM for the $In_xGa_{1-x}N$ films with different In contents.

3. Results and discussion

Fig. 1a and b shows the normalized PL spectra of $In_xGa_{1-x}N$ films with different In contents at 300 and 12 K, respectively. Here, the normalization is with respect to the peak intensity of the PL feature. In Fig. 1a, peak energies of the PL signals measured at 300 K are estimated to be 3.35, 3.29, 2.99, 2.99, 2.59, 2.31 eV for the sample with $x = 0.02$, 0.04, 0.11, 0.15, 0.30 and 0.33, respectively. In the present analysis, we assume that the band-gap of InGaN can be directly obtained from the maximum of the PL peaks. The obtained band-gap of the InGaN samples as a function of In content are then plotted in Fig. 2.

It has been known that the band-gap values for a ternary compound $A_xB_{1-x}C$ do not vary linearly with the band-gap values of the two binary ends, $E_{g,AC}$ and $E_{g,BC}$ The variation for the band-gap of $In_xGa_{1-x}N$ is more appropriately described by [5,17,18]:

$$E_{g,\mathrm{InGaN}}(x) = xE_{g,\mathrm{InN}} + (1-x)E_{g,\mathrm{GaN}} - bx(1-x) \quad (1)$$

where b is the bowing parameter and has units of energy. In Fig. 2, the red[1] solid line is the theoretical line least squared fit to Eq. (1) using the reported values of $E_{g,InN} = 0.7$ eV, $E_{g,GaN} = 3.4$ eV, with the bowing parameter b estimated to be 1.36 eV. The value is very similar to the obtained value of 1.43 for In-rich InGaN [17], and is in agreement with the recent calculations predicting a value of 1.36 eV for the whole composition range [18]. However, a slight deviation from Eq. (1) is observed for InGaN samples with $x > 0.11$, which can be attributed to a larger degree of compositional inhomogeneity in In distribution for the In-rich samples [17,18].

From the 12 K PL spectra (Fig. 1b), it can be observed that the PL shape tends to become asymmetric with a low energy tail and increased FWHM with increasing In content >0.11. The relationship between the degree of compositional fluctuation and the broadened PL features as a function of In content is analyzed as follows. The estimated FWHM as a function of In content are plotted as opened squares in Fig. 3, and the theoretical variation in the FWHM, ΔE_{EXC}, of the PL peaks can be described by [19,20].

$$\Delta E_{\mathrm{EXC}} = 2.36\sigma_E \quad (2)$$

where σ_E is the standard deviation of the band gap energy given by [20].

[1] For interpretation of color in Figs. 2 and 4, the reader is referred to the web version of this article.

Author's personal copy

$$\sigma_E = |\frac{dE_g(x)}{dx}|\sqrt{\frac{x(1-x)}{4a_0^{-3}(\frac{4}{3})\pi a_{exc}^3}} \quad (3)$$

In Eq. (3), $\frac{dE_g(x)}{dx} = 2.72x - 4.06$ describes the variation of the band gap with composition, $a_0 = 0.3189x + 0.3548(1-x)$ nm [21] is the lattice constant for the ternary alloy, and a_{exc} is the Bohr radius of the exciton. The exciton Bohr radius a_{exc} can be estimated from a scaled hydrogen model to be $a_{exc} = a_B^H \varepsilon(x)\frac{m_0}{\mu}$ [22] with a_B^H being the Bohr radius of the hydrogen atom, $\varepsilon(x) = 10.5x + 8.9(1-x)$ is the x-dependent static dielectric constant of $In_xGa_{1-x}N$, m_0 is the free electron mass, and $\mu = (1/m_e + 1/m_h)^{-1}$ is the exciton reduced mass with $m_e = 0.2m_0$ and $m_h = 1.1m_0$ [21,23] being the electron and hole masses, respectively.

The theoretical curve as a function of x given by Eq. (2) is shown as the dotted line in Fig. 3. However, the theoretical curve is lower than the measured FWHM values. Nevertheless, the FWHM data for the samples with $x < 0.15$ can be well fitted by a modified relation with $2.8\Delta E_{EXC}$ and is plotted as the solid line in Fig. 3. A possible explanation is related to the Bohr radius of exciton, which is a critical parameter for calculating the excitonic volume in InGaN material. Therefore, the larger ΔE_{EXC} indicates that the actual exciton Bohr radius in our samples has to be smaller than that of the theoretical value as given by Ref. [22]. It should also be noted that the $In_xGa_{1-x}N$ samples with $x = 0.30$ and 0.33 have exhibited exceedingly large FWHM values as depicted in Fig. 3. Chichibu et al. and Yamamoto et al. indicated that the large FWHM value is not only caused by the statistical compositional fluctuation, but also by the excitonic localization effect, which has its origin from the phase separation due to larger alloy compositional fluctuation in the In-rich InGaN films [11,24]. The phase separation in the InGaN films with higher In content plays a pronounced role in nitride-based material LEDs. The samples contain regions of higher In content (smaller band gap) embedded in regions with higher Ga content (higher band gap). The main PL feature may accompany by several lower PL peaks (as clearly indicated by the PL feature for In content of 0.3 in Fig. 1) rendering the overall PL structure to appear broadened and asymmetric [25,26], and this explained the much larger FWHM for InGaN with In content of 0.30 and 0.33.

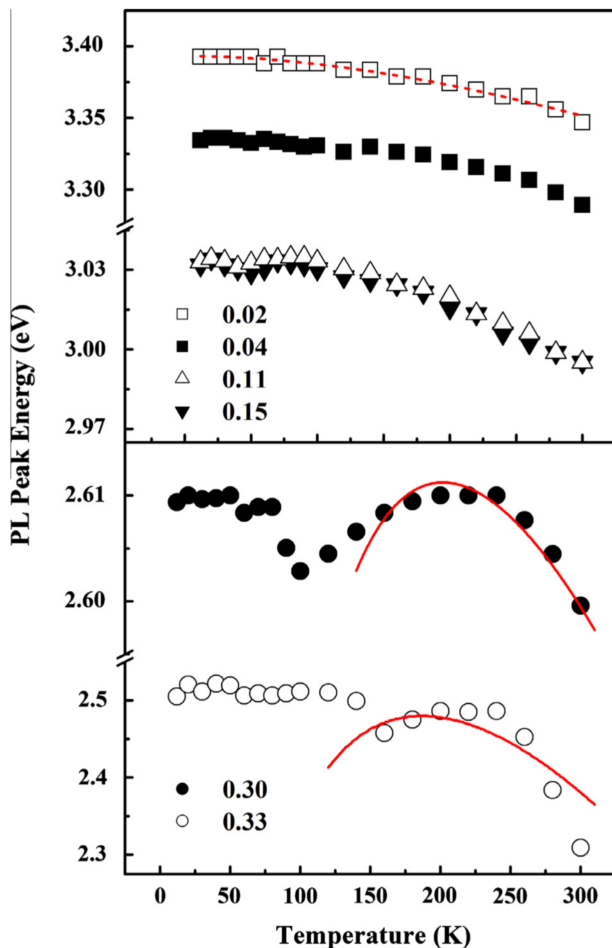

Fig. 4. Temperature dependence of PL peak position for the $In_xGa_{1-x}N$ films with different In contents.

To study the exciton localization effect as a function of In content, the temperature dependence of the PL peak energy of InGaN samples is plotted in Fig. 4. The variation for the InGaN with In content of 0.02 exhibits a typical redshift with increasing temperature, and can be described by the Varshni expression [19]:

$$E(T) = E(0) - \frac{\alpha T^2}{T+\beta} \quad (4)$$

where $E(0)$ is the exciton energy at $T = 0$ K, and α and β are fitting parameters. The red dashed line in Fig. 4 for In content of 0.02 show that the experimental data can be fitted well by Eq. (4) with $E(0) = 3.39$ eV, $\alpha = 0.53$ meV/K, and $\beta = 850$ K. However, by increasing the In content above 0.11, it is observed that the band gap variation with temperature deviates from the Varshni relation. As a function of temperature, the PL peak redshifts slightly in the low temperature region, and then blueshifts in the intermediate temperature region, and again redshifts till room temperature is reached. The anomalous temperature dependence of luminescence peak position has been referred as S-shaped dependence. It is evident that the S-shaped behavior would become more pronounced for increasing In content and especially so for InGaN with In contents of 0.30 and 0.33.

It has been known that the exciton dynamic as a function of temperature results in the S-shaped emission shift (decrease–increase–decrease) in PL peak energy. At very low temperature, the excitons are frozen out at the local minima. Initial increase of the temperature resulting in the excitons acquiring sufficient thermal energy to overcome the small potential barriers in the local potential and relax to the absolute potential minimum, thus the PL peak energy exhibits redshift. By increasing the temperature further, the excitons can be thermally transferred to higher energy states until reaching the conduction-band edge, which result in the spectral blueshift. With any further increases in temperature, the thermal ionization effect prevents the exciton localization and results in spectral redshift again. Therefore, the temperature variation of the band gap as given by the Varshni's expression should be modified to include the exciton localization effect and can be written as [27,28]:

$$E(T) = E(0) - \frac{\alpha T^2}{T+\beta} - \frac{\sigma^2}{K_B T} \quad (5)$$

where K_B is the Boltzmann's constant and σ is the excitonic localization energy. The experimental PL peak energies variation with temperature for 30% and 33% In contents are then fitted by Eq. (5) and plotted as the red solid line in Fig. 4. The estimated σ values are about 29 and 65 meV for $In_xGa_{1-x}N$ with $x = 0.3$ and 0.33, respectively. The larger σ value means stronger exciton localization. Our study shows large compositional fluctuation in In-rich InGaN leading to phase separation, which yields the observed S-shaped PL emission behavior.

The results of our temperature-dependent PL study are well supported by the SEM images taken for the as-grown InGaN samples. The SEM images showing the surface morphology for a few

Author's personal copy

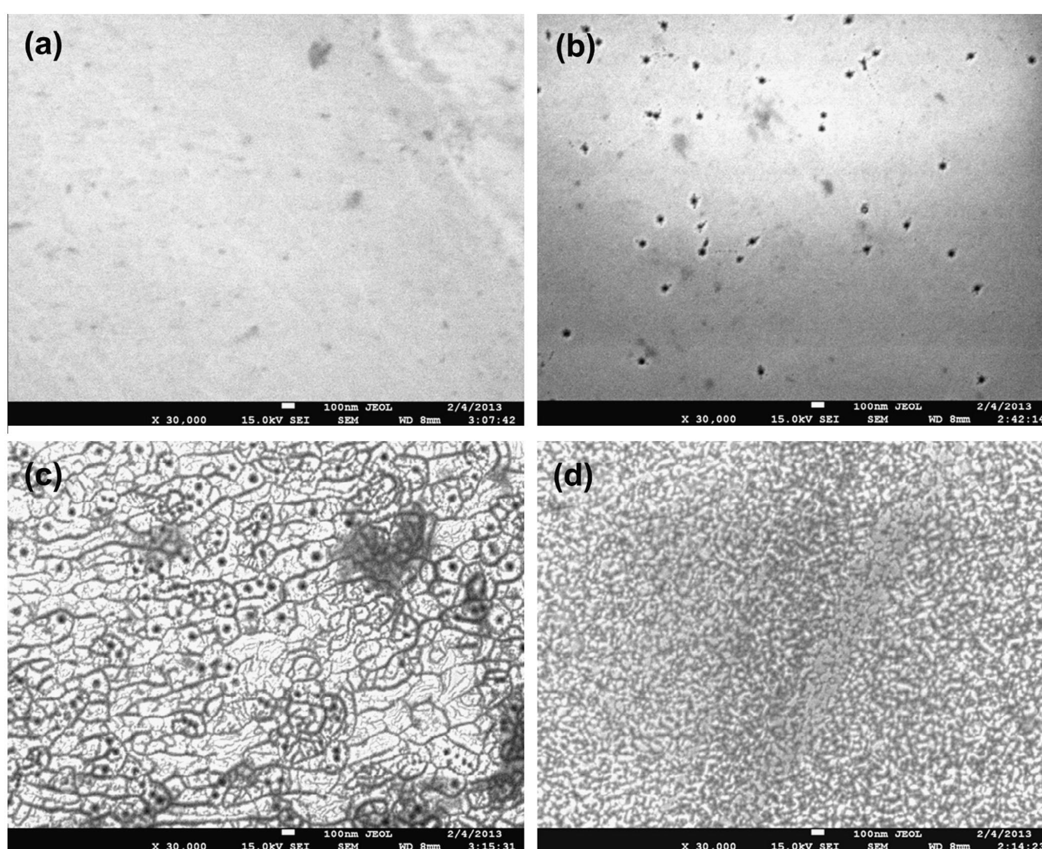

Fig. 5. SEM images for the $In_xGa_{1-x}N$ films with In content; (a) 0.02, (b) 0.15, (c) 0.30, and (d) 0.33.

representative samples with $x = 0.02$, 0.15, 0.30 and 0.33 are included as Fig. 5. The SEM images clearly indicated a relatively smooth and homogeneous surface for samples with small In content of 0.02. As the In content is increased to 0.15, non-uniform distribution of dark pits begins to appear. At $x = 0.30$ and 0.33, the SEM images show extensive inhomogeneous distribution of In islands on the surface of the as-grown samples [29,30]. Zhao et al. have indicated that more In atoms can diffuse into the islands because the diffusion capability of In adatoms is higher than that of Ga adatoms. Since more In atoms combine into the islands for the In-rich InGaN, In compositional inhomogeneity caused by phase separation is facilitated in the islands [30].

4. Conclusion

In summary, the luminescence properties of $In_xGa_{1-x}N$ with different In content ($x = 0.02, 0.04, 0.11, 0.15, 0.30$ and 0.33) are analyzed in detail by temperature-dependent PL. The variation in the FWHM values of InGaN as a function of In content indicates that the compositional fluctuation due to the inhomogeneous In distribution being responsible for the broadening in FWHM. It is also observed that the S-shaped temperature dependence of the PL peak of InGaN films becomes more significant with increasing In content indicating a stronger localization effect in the InGaN with increasing In content. Additionally, an emission mechanism originating from the phase separated In-rich region should be taken into account to describe the much larger FWHM and S-shaped emission shift for the InGaN with In content of 0.30 and 0.33. The results of the temperature-dependent PL are correlated well with SEM images showing the surface morphology of the as-grown samples.

Acknowledgement

The author would like to acknowledge the support of the National Science Council Project No. NSC 99-2112-M-236-001-MY3.

References

[1] A. Gauthier-Brun, J.H. Teng, E. Dogheche, W. Liu, A. Gokarna, M. Tonouchi, S.J. Chua, D. Decoster, Appl. Phys. Lett. 100 (2012) 071913.
[2] O. Lupan, T. Pauporté, B. Viana, Adv. Mater. 22 (2010) 3298.
[3] G. Simin, X. Hu, A. Tarakji, J. Zhang, A. Koudymov, S. Saygi, J. Yang, A. Khan, M.S. Shur, R. Gaska, Jpn. J. Appl. Phys. 40 (2011) L1142.
[4] L. Sang, M. Liao, Y. Koide, M. Sumiya, Appl. Phys. Lett. 98 (2011) 103502.
[5] Md. Rafiqul Islam, Md. Rejvi Kaysir, Md. Jahirul Islam, A. Hashimoto, A. Yamamoto, J. Mater. Sci. Technol. 29 (2013) 128.
[6] A. Gokarna, A. Gauthier-Brun, W. Liu, Y. Androussi, E. Dumont, E. Dogheche, J.H. Teng, S.J. Chua, D. Decoster, Appl. Phys. Lett. 96 (2010) 191909.
[7] M. Moret, B. Gil, S. Ruffenach, O. Briot, Ch. Giesen, M. Heuken, S. Rushworth, T. Leese, M. Succi, J. Cryst. Growth 311 (2009) 2795.
[8] C.Z. Zhao, R. Zhang, B. Liu, D.Y. Fu, H. Chen, M. Li, Z.L. Xie, X.Q. Xiu, S.L. Gu, Y.D. Zheng, Sci. China – Phys. Mech. Astron. 55 (2012) 396.
[9] K. Kazlauskas, G. Tamulatis, S. Juršėnas, A. Žukauskas, M. Springis, Y.C. Cheng, H.C. Wang, C.F. Huang, C.C. Yang, Phys. Stat. Sol.: C 2 (2005) 1023.
[10] V. Kachkanov, K.P. O'Donnell, S. Pereira, R.W. Martin, Phil. Mag. Lett. 87 (2007) 1999.
[11] S. Chichibu, T. Azuhata, T. Sota, S. Nakamura, Appl. Phys. Lett. 70 (1997) 2822.
[12] C. Sasaki, H. Naito, M. Iwata, H. Kudo, Y. Yamada, T. Taguchi, T. Jyouichi, H. Okagawa, K. Tadatomo, H. Tanaka, Phys. Stat. Sol.:C (2002) 320.
[13] H.S. Chang, T.M. Hsu, T.F. Chuang, W.Y. Chen, S. Gwo, C.H. Shen, Solid State Commun. 149 (2009) 18.
[14] Q. Li, S.J. Xu, M.H. Xie, S.Y. Tong, J. Phys.: Condens. Matter 17 (2005) 4853.
[15] Z.C. Feng, W. Liu, S.J. Chua, J.W. Yu, C.C. Yang, T.R. Yang, J. Zhao, Thin Solid Films 498 (2006) 118.
[16] W. Shan, W. Walukiewicz, E.E. Haller, B.D. Little, J.J. Song, M.D. McCluskey, N.M. Johnson, Z.C. Feng, M. Schurman, R.A. Stall, J. Appl. Phys. 84 (1998) 4452.
[17] J. Wu, W. Walukiewicz, K.M. Yu, J.W. Ager, E.E. Haller, Hai Lu, William J. Schaff, Appl. Phys. Lett. 80 (2002) 4741.
[18] P.G. Moses, C.G.V. de Walle, Appl. Phys. Lett. 96 (2010) 021908.

Author's personal copy

[19] G.R. James, A.W.R. Leitch, F. Omnes, M. Leroux, Semicond. Sci. Technol. 21 (2006) 744.
[20] J. Hellara, F. Hassen, H. Maaref, H. Dumont, V. Souliere, Y. Monteil, Microelectron. J. 35 (2004) 207.
[21] Y.M. Chi, J.J. Shi, Chin-Phys. Lett. 23 (2006) 2206.
[22] S. Heitsch, G. Zimmermann, D. Fritsch, C. Sturm, R. Schmidt-Grund, C. Schulz, H. Hochmuth, D. Spemann, G. Benndorf, B. Rheinländer, Th. Nobis, M. Lorenz, M. Grundmann, J. Appl. Phys. 101 (2007) 083521.
[23] G.F. Brown, J.W. Ager III, W. Walukiewicz, J. Wu, Sol. Energy Mater. Sol. C. 94 (2010) 478.
[24] K. Yamamoto, T. Tsuboi, T. Ohashi, T. OTawara, H. Gotoh, A. Nakamura, J. Temmyoa, J. Crystal. Growth 312 (2010) 1703.
[25] B.N. Pantha, J. Li, J.Y. Lin, H.X. Jiang, Appl. Phys. Lett. 96 (2010) 232105.
[26] Z.Z. Chen, Z.X. Qin, X.D. Hu, T.J. Yu, Z.J. Yang, Y.Z. Tong, X.M. Ding, G.Y. Zhang, Physica B 344 (2004) 292.
[27] A. Bell, S. Srinivasan, C. Plumlee, H. Omiya, F.A. Ponce, J. Christen, S. Tanaka, A. Fujioka, Y. Nakagawa, J. Appl. Phys. 95 (2004) 4670.
[28] S.A. Lourenço, M.A.T. da Silva, I.F.L. Dias, J.L. Duarte, E. Laureto, A.A. Quivy, T.E. Lamas, J. Appl. Phys. 101 (2007) 113536.
[29] H. Komaki, T. Nakamura, R. Katayama, K. Onabe, M. Ozeki, T. Ikari, J. Crystal Growth 301–302 (2007) 473.
[30] W. Zhao, L. Wang, J.X. Wang, Y. Luo, Chin. Phys. B 20 (2011) 076101.